

## Use of Two-Dimensional and Three-Dimensional Reactors in Oxidative Electrochemical Degradation Studies of Malachite Green

Canan Samdan<sup>1\*</sup> 

<sup>1\*</sup> Eskisehir Osmangazi University, Faculty of Engineering and Architecture, Department of Chemical Engineering, Eskişehir, Türkiye, [caydin@ogu.edu.tr](mailto:caydin@ogu.edu.tr)

\*Corresponding Author

### ARTICLE INFO

### ABSTRACT

#### Keywords:

Electrochemical  
oxidative degradation  
Microelectrodes  
Malachite green



#### Article History:

Received: 14.05.2023

Accepted: 21.11.2023

Online Available: 27.02.2024

With the developments in treatment technologies, including porous materials in electrochemical systems have recently become the focus of researchers' attention. In electrochemical methods, operating cost is as important as efficiency. It is possible to increase the system performance by increasing the effective electrode surface by incorporating activated carbon, which can be produced from biomass, into electrochemical oxidation systems. This study investigated using activated carbon from walnut shells as a microelectrode in the electrochemical oxidative degradation of malachite green. When potential differences between 2V and 4V are applied to 2DES and 3DES reactors containing MG solution, a higher % MG Removal was obtained in 3DES reactors than in 2DES reactors. When the potential difference is 4V, a value of  $0.026 \text{ (min}^{-1}) k_{1,3D}$  and  $0.0117 \text{ (min}^{-1}) k_{1,2D}$  are obtained. In 3DES reactors, the rate constant at  $0.003 \text{ A/cm}^2$  was achieved as  $0.0167 \text{ (min}^{-1}) k_{1,3D}$ , while at  $0.010 \text{ A/cm}^2$ , it increased by approximately 5 times, reaching a value of  $0.0845 \text{ min}^{-1} k_{1,3D}$ . Similarly, in 3DES reactors, when the current density increased from  $0.003 \text{ A/cm}^2$  to  $0.010 \text{ A/cm}^2$ , the mass transfer rate increased from  $0.011 \text{ (cm/s)}$  to  $0.05633 \text{ (cm/s)}$ .

## 1. Introduction

Electro-oxidation is a method by which hydroxyl radicals oxidize and purify pollutants. It is one of the most widely used methods in wastewater treatment as it allows the breakdown of high-toxicity waste [1]. The anode has an essential place in the electro-oxidation method. In studies with electro-oxidation processes (2DES), generally, Ti/Ru TiO<sub>2</sub>, Ti/Pt [2], Ti/Ir-Pb, Ti/Ir-Sn, Ti/Ru-Pb, Ti/Pt-Pd and Ti/RuO<sub>2</sub> [3] etc. anodes are widely used. Particle electrodes are essential in designing and operating three-dimensional electrochemical oxidative degradation reactors (3DES). It has many advantages over traditional electrochemical oxidation reactors and has become the focus of interest of researchers since its inception. Recently, many studies have focused on

preparing particle electrodes for 3D electrochemical oxidation [4,5].

Particle electrodes are mainly prepared using highly porous and high-impedance materials. Researchers have used various materials, such as graphite [6], Ti-Sn/ $\gamma$ -Al<sub>2</sub>O<sub>3</sub> [7], CuFe<sub>2</sub>O<sub>4</sub> [8], Pd-supported magnetic biochar [9],  $\gamma$ -Fe<sub>2</sub>O<sub>3</sub>-CNTs [10] and activated carbon [11] in the synthesis of particle electrodes. However, developing such particle electrodes is limited due to the complex preparation process and expensive (or non-abundant) raw materials, which hinders the practical application of the 3-D electrochemical oxidation reactor. Therefore, selecting available and cost-effective raw materials for the preparation of particulate electrodes is crucial. Therefore, synthesizing particle electrodes using local and abundant waste biomass is a very logical method.

The 3D electro-oxidation method, based on traditional electrochemical technology, is developed by filling conductive particles between the anode and the cathode [12]. The 2-dimensional electro-oxidation method is the realization of the electro-oxidation process on a thin film on the surface of an electrode. In the 3D electro-oxidation method, it is possible to increase the surface of the microelectrodes easily by increasing the amount of particle electrodes. In this way, the surface area where direct oxidation will occur is increased. This situation improves the degradation of the pollutant to be removed [8].

This study examined the oxidative degradation of malachite green (MG) using activated carbons produced from biomass kinetically in a 3D electro-oxidation reactor. At the same time, the degradation of malachite green was performed in the 2D electro-oxidation reactor, and the kinetic results were compared with the 3D reactor.

## 2. Materials And Method

### 2.1. Devices and chemicals

Phosphoric acid ( $\text{H}_3\text{PO}_4$ ) (Merck) was used for the chemical activation process of biomass to produce activated carbon with an acidic character. The pH values of the solutions were brought to the desired value by using 0.1N HCl (Merck) and 0.1N NaOH pellets (Merck EMPLURA®) solutions. The malachite green (basic green 4) was used as an organic compound. UV/vis spectrophotometer (Model: Thermo Electron AquaMete) was used to measure the MG concentration in aqueous solution.

### 2.2. Production of activated carbons as microparticles

Walnut shells were ground into small pieces. Walnut shells and the appropriate amount of  $\text{H}_3\text{PO}_4$  were added as a walnut shell/ $\text{H}_3\text{PO}_4$  ratio (w/w) of 4/1. This mixture was mixed with a magnetic stirrer at 65 °C for 7 hours; the heating was turned off and left for 17 hours. The filtered sample was dried in an oven. The appropriate amount from the sample, which absorbed the chemical agent, was placed in the reaction vessel.

The vessel was brought to 400 °C in a nitrogen atmosphere. The reactor was kept at the final temperature for 1 hour and was left to cool in the furnace. Micro and mesoporous activated carbon with 1328  $\text{m}^2/\text{g}$  surface area was produced using 4/1 (w/w) phosphoric acid from the walnut shell. Activated carbon is used as microelectrodes in 3DES reactors.

### 2.3. Electrochemical oxidative degradation

In this study, a three-dimensional electrode system (3DES) and a two-dimensional electrode system (2DES) were used as electrochemical (EC) oxidative degradation systems. A schematic image of 2DES and 3DES electro-oxidation systems is given in Figure 1. For this purpose, a 5x10x5 mm glass electrolytic cell connected to a DC power source and continuously stirred was used in 2DES and 3DES systems.

Carbon fibre was used as an anode and cathode for 2.5x2.5 cm (6.25  $\text{cm}^2$  surface area). While the 2DES electrochemical cell was designed with an anode and cathode, activated carbon was added between the anode and the cathode in the 3DES cell, and 0.2 g activated carbon was used as particle electrodes. Each 3DES reactor has a surface area of 265.6  $\text{m}^2$  (1328  $\text{m}^2/\text{g}$  particle electrode x 0.2 g particle electrode) of particulate electrodes. A 3-phase, 3-dimensional electrochemical oxidation system is built in the 3DES cell, where continuous mixing is applied. The voltage during the 2DES and 3DES experiments was varied in the range of 2-4 V.

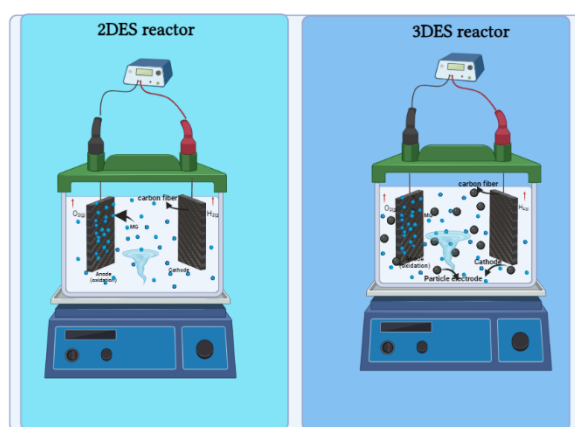


**Figure 1.** Schematic image of 2DES and 3DES systems

0.003-0.010 (A/cm<sup>2</sup>) j values were applied. All experiments were carried out under control during the study at 25 °C. MG solutions were loaded into the EC reactor at an initial concentration of 250 ppm in each EC experiment. Sodium chloride was used to adjust the initial conductivity of the solution. During the experiments, 2 ml samples were drawn from the solution and analyzed to determine the amount of MG.

A calibration curve was created in a UV-vis spectrophotometer using MG solutions at different concentrations. The concentration of MG in the solution at any time was calculated using this calibration curve at 621 nm [13]. Using the MG concentration (C) in the solution at any time t and the MG concentration (C<sub>0</sub>) at time t = 0, the % MG Removal was calculated using Eq 1.

$$\% \text{ Removal} = \frac{C}{C_0 - C} * 100 \quad (1)$$

If we consider electro-oxidation as a surface treatment, then the kinetics of decay can be represented by the following Eq. 2 in terms of the heterogeneous rate constant, k<sub>h</sub> (cm/s) [14],

$$r = - \left( \frac{V}{A_e} \right) \frac{d[C]}{dt} = k_h [C] \quad (2)$$

Where A<sub>e</sub> electrode surface area (cm<sup>2</sup>), V is the reactor volume (cm<sup>3</sup>), and t is the EC oxidative degradation time (s). Inside the electro-oxidation reactor, the MG removal rate is proportional to the concentration of the contaminant. Therefore, the kinetics for MG removal can be represented by the following pseudo-first-order kinetic model: Eqs. (3 and 4) [15,16]:

$$r = - \frac{d[C]}{dt} = k_{1 \text{ 2D or 3D}} [C] \quad (3)$$

$$-\ln \left( \frac{C}{C_0} \right) = k_{1 \text{ 2D or 3D}} t \quad (4)$$

Where k<sub>1 2D or 3D</sub> is the pseudo-first-order reaction rate constant (min<sup>-1</sup>), and k<sub>1 2D or 3D</sub> is related to k<sub>h</sub> as follows Eq. 5. Constants can be determined from ln (C/C<sub>0</sub>) vs time graphs.

$$k_h = k_{1 \text{ 2D or 3D}} \left( \frac{V}{A_e} \right) \quad (5)$$

### 3. Results And Discussion

#### 3.1. Textural properties of particle electrodes

The surface area, micropore volume, mesopore volume and average pore diameter obtained using N<sub>2</sub> adsorption-desorption isotherms of particle electrodes are given in Table 1.

**Table 1.** The surface pore properties of the particle electrodes

S <sub>BET</sub> (m <sup>2</sup> /g)	V <sub>mic</sub> (cm <sup>3</sup> /g)	V <sub>mes</sub> (cm <sup>3</sup> /g)	V <sub>tot</sub> (cm <sup>3</sup> /g)	D <sub>p</sub> (Å)
1328	0.492	0.286	0.778	23.44

The surface area of particle electrodes is 1328 m<sup>2</sup>/g, and its total pore volume is 0.778 cm<sup>3</sup>/g. The micropore volume is more than the mesopore volume. The average pore diameter is 23.44 Å. Adsorption-desorption isotherms and pore size distributions of particle electrodes are given in Figure 2.

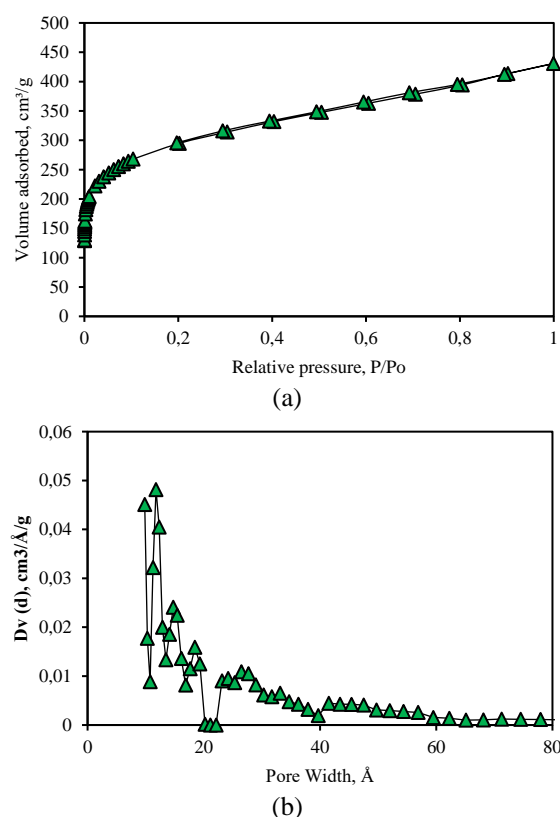


**Figure 2.** Adsorption-desorption isotherms (a) and pore size distributions (b) of particle electrodes

Considering Figure 2 (a), the adsorption-desorption isotherms of particle electrodes comply with Type I isotherms according to the IUPAC classification [17]. According to Figure 2 (b), the particle electrodes had peaks between 10-20 Å (1-2 nm) and 20-60 Å (2-4 nm). According to IUPAC, the pores of porous materials such as activated carbon are classified as micropores (<2 nm), mesopores (2-50 nm), and macropores (> 50 nm). In this study, particle electrodes consist of micro and mesopores.

2DES and 3DES reactors were used in MG oxidative electrochemical degradation studies. The effects of voltage and current densities applied to the reactors were investigated to determine the reactor efficiency.

### 3.2. Effect of voltage

In the experiments with 2D and 3D electrochemical (EC) oxidative degradation systems, the MG concentration changes occurring at all potential difference values examined during the reaction were recorded and shown graphically in

. The resulting energy consumption values were calculated with the help of these values and shown graphically in Figure 4. The energy consumption values obtained with the help of the potential difference values that occur during the reaction were calculated with the help of (6) [18].

$$E = \frac{U \cdot I \cdot t}{V} \quad (6)$$

Where E is electrical energy (kWh/m<sup>3</sup>), U is volts, I is current intensity (A), t is time (hours), and V is solution volume (m<sup>3</sup>). Energy consumption is also calculated according to (7) per unit mass of decomposed MG [19].

$$E = \frac{U \cdot I \cdot t}{(C_0 - C) \cdot V} \quad (7)$$

Where E is electrical energy (kWh/g MG), U is volt, I is current intensity (A), t is time (hours), V is solution volume (L). While calculating the energy consumption values, the current densities for 2, 3, and 4V potential differences in 2DES reactors were taken as 0.033, 0.044 and 0.057 A/cm<sup>2</sup>, respectively. In 3DES reactors, the

current densities for the same potential differences are 0.060, 0.067 and 0.081 A/cm<sup>2</sup>, respectively.

According to Figure 3, when potential differences between 2V and 4V are applied to 2DES and 3DES reactors containing MG solution, a higher % MG Removal was obtained in 3DES reactors than in 2DES reactors. Direct oxidation of MG takes place in two steps: the first is the diffusion of MG to the anode surface, and the second is the oxidation of MG on the anode surface. In 3DES reactors, microelectrodes provide an extra surface for the oxidation of MG molecules. In this way, more MG molecules are degraded due to electron transfers occurring both on the carbon fibre surface, which is the anode, and on the surface of the microelectrodes. When the 3DES reactors are not subjected to any potential difference (0 V), the MG molecules that come into contact with the particle electrodes are absorbed on the surfaces of the particle electrodes. Without a potential difference, the adsorption mechanism results in a 13.87% MG Removal.

When the potential difference in the 2DES reactor increased from 2V to 4V, the %R value increased from 65.74 to 76.00. Similarly, in 3DES reactors, with the potential difference increase to 3V, the %R value increased from 87.6 to 95.6. When 4V voltage was applied in 3DES reactors, a 96.8 %R value was obtained. The variation of the same potential difference reduced the normalized concentration from 0.34 to 0.20 in 2DES reactors and from 0.12 to 0.032 in 3DES reactors at 120 min. The optimum potential difference was considered 3V since the decomposition efficiencies obtained at the 3V and 4V potential differences were close. However, the results also need to be evaluated from an economic point of view. As seen in Eq. (6), the energy consumption value is expressed as the amount of energy applied per unit of time per unit volume. The potential difference value applied to the system is one of the critical parameters affecting energy consumption. The increase in the value of the potential difference applied causes the energy consumption value to increase. For all the potential differences studied, 3DES reactors consumed more energy than 2DES (Figure 4 (a)).

At 4V volts, where the highest MG removal values were obtained, 11.52 kWh/m<sup>3</sup> energy consumption was a requirement in 2DES reactors, while 16.32 kWh/m<sup>3</sup> energy was needed in 3DES reactors. The microelectrodes used in 3DES reactors have caused electrical resistance in the system.

The increase in resistance led to an increase in current at a constant voltage. As a result, 3DES reactors have higher energy requirements.

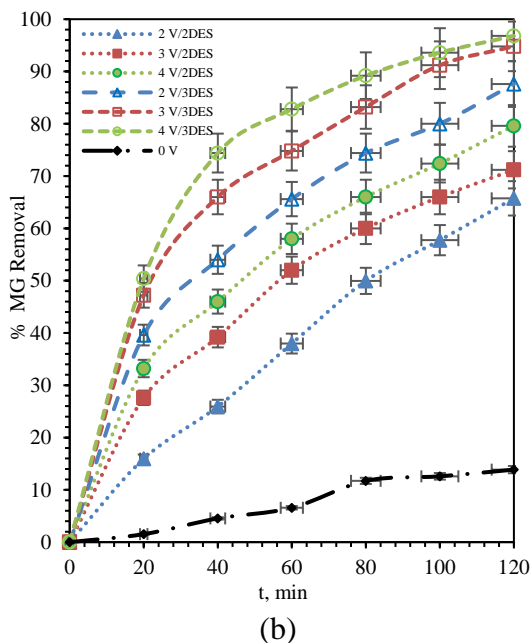
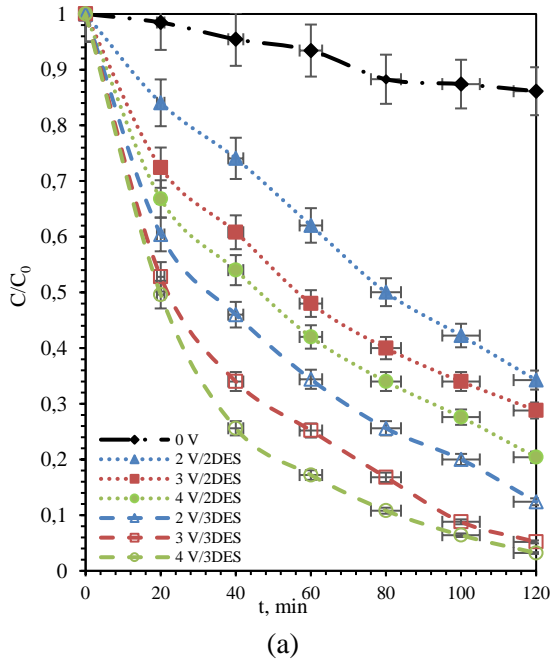


**Figure 3.** Comparison of normalized concentration vs time (a) and % MG Removal vs time (b) at different potentials in 2DES and 3DES oxidation systems

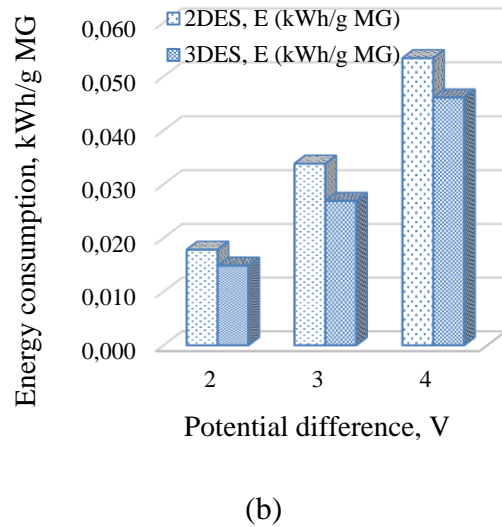
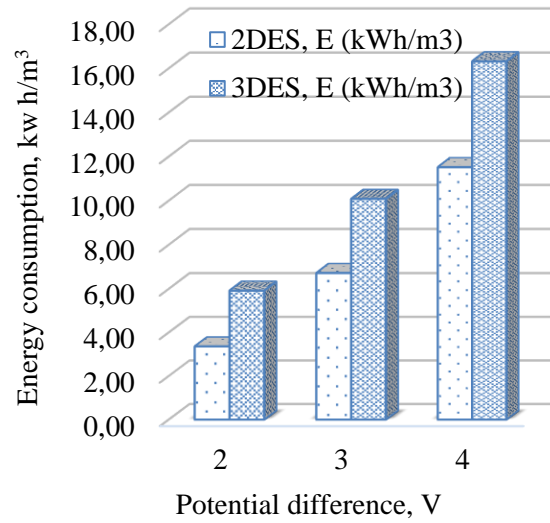


**Figure 4.** The resulting energy consumption values for 2DES and 3DES reactors

When the energy requirements per gram of the degraded MG are examined (Figure 4 (b)), the energy requirement in 3DES reactors is lower than in 2DES reactors. In 3DES reactors, the energy consumption of 0.015, 0.028 and 0.048 kWh/gMG was realized for potential differences of 2, 3 and 4V. In 2DES reactors, the energy consumption of 0.020, 0.038, and 0.061 kWh/gMG occurred for the same potential differences. From this point of view, 3DES reactors are more economical. When the 3D electrochemical oxidative degradation system

was evaluated regarding energy consumption to determine the optimal potential difference, less energy requirement occurred in 3V than in 4V. Therefore, the 3V potential difference may be the optimum condition for 3DES reactors.

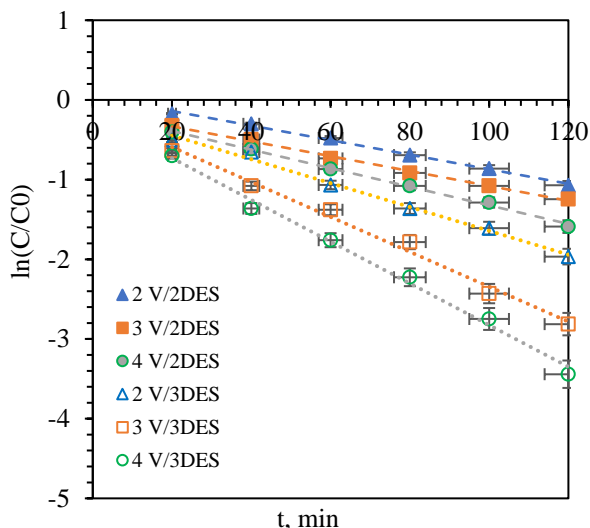


**Figure 5.** The pseudo-first-order kinetic model for 2DES and 3DES reactors at 2V, 3V and 4V

To kinetically evaluate the data obtained at 2, 3 and 4V potential differences,  $\ln(C/C_0)$  - time graphs were drawn for 2DES and 3DES reactors and pseudo-first-order reaction rate constants  $k_{1,2D}$  ( $\text{min}^{-1}$ ) and  $k_{1,3D}$  ( $\text{min}^{-1}$ ) were calculated. The resulting graphs are shown in Figure . In addition, the  $k_h$  (cm/s) values for the MG degradation reactions in the 2DES and 3DES reactors (Eq. (5)) are calculated, and all rate constants are given in Table 2.

As the voltage increased in 2DES reactors, the oxidative degradation rate increased, and the highest values of  $k_{1,2D}$  and  $k_{h,2D}$  were obtained as 0.0117 ( $\text{min}^{-1}$ ) and 0.0078 (cm/s) at 4V, respectively. In 3DES reactors, when a potential difference of 2V is applied, a value of 0.015 ( $\text{min}^{-1}$ )  $k_{1,3D}$  is obtained, while when the potential difference is increased to 4V, a value of 0.026 ( $\text{min}^{-1}$ )  $k_{1,3D}$  is obtained. In addition, the heterogeneous rate constant increased as the potential difference applied increased.

### 3.3. Effect of current density

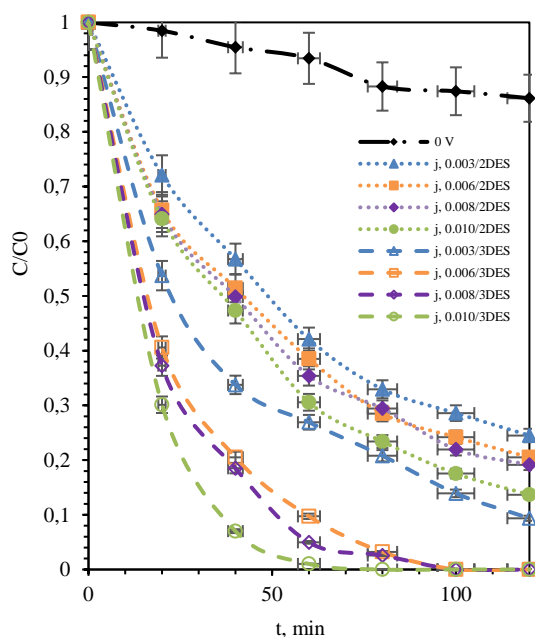
To investigate the effect of current density on the oxidative degradation of MG, experiments were performed in both 2DES and 3DES reactors at

different current densities. Over time, the oxidative degradation rate and % degradation amount of MG were determined, and the results are given in Figure 6. The compatibility of the obtained data with the pseudo-first-order kinetic model was investigated (Figure 7). The pseudo-first-order rate constant ( $k_{1,2D}$  ( $\text{min}^{-1}$ ) and  $k_{1,3D}$  ( $\text{min}^{-1}$ )) and heterogeneous rate constants ( $k_{h,2D}$  (cm/s) and  $k_{h,3D}$  (cm/s)) for both reactor types are calculated and given in Hata! Başvuru kaynağı bulunamadı..

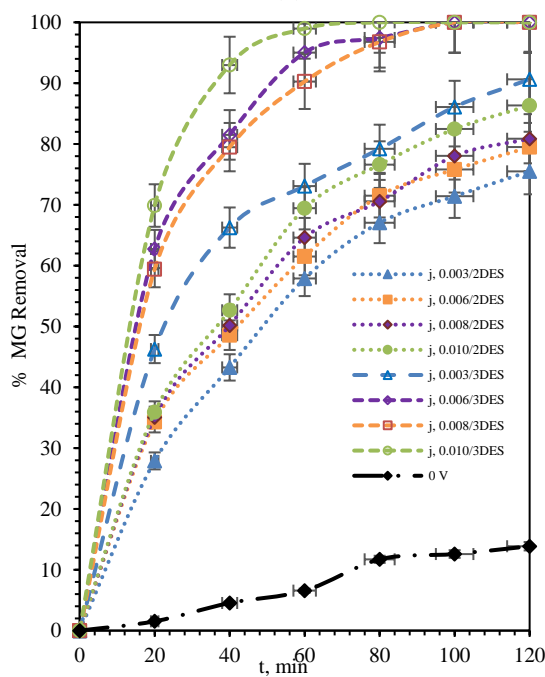
**Table 2.** Kinetic rate constants for electro-oxidative degradation of MG in 2DES and 3DES reactors

2DES			
V (volt)	$k_{1,2D}$ ( $\text{min}^{-1}$ )	$k_{h,2D}$ (cm/s)	$R^2$
2V	0.0091	0.00607	0.99
3V	0.0093	0.00620	0.99
4V	0.0117	0.00780	0.99
j (A/cm <sup>2</sup> )	$k_{1,2D}$ ( $\text{min}^{-1}$ )	$k_{h,2D}$ (cm/s)	$R^2$
0.003	0.0110	0.00733	0.98
0.006	0.0118	0.00787	0.99
0.008	0.0125	0.00833	0.98
0.010	0.0157	0.01047	0.99
3DES			
V (volt)	$k_{1,3D}$ ( $\text{min}^{-1}$ )	$k_{h,3D}$ (cm/s)	$R^2$
2V	0.015	0.0100	0.99
3V	0.022	0.0146	0.98
4V	0.026	0.0173	0.99
j (A/cm <sup>2</sup> )	$k_{1,3D}$ ( $\text{min}^{-1}$ )	$k_{h,3D}$ (cm/s)	$R^2$
0.003	0.0167	0.01113	0.99
0.006	0.0418	0.02787	0.98
0.008	0.0467	0.03113	0.98
0.010	0.0845	0.05633	0.99

As the current density applied in the 2DES and 3DES reactors increased, the normalized concentration value decreased from 0.24 to 0.13 in 2DES reactors and decreased from 0.09 to 0 in 3DES reactors (Figure 6 (a)). Similarly, the % MG Removal value increased (Figure 6 (b)).



(a)



(b)

**Figure 6.** Comparison of normalized concentration vs time (a) and % MG Removal vs time (b) at different current densities in 2DES and 3DES oxidation systems

At the end of 2 hours in 2DES reactors, 75.50% MG Removal was achieved at 0.003 A/cm<sup>2</sup> current density, and 86.33% %R value was obtained at 0.010 A/cm<sup>2</sup>. In 3DES reactors, 90.63% MG Removal was achieved at 0.003 A/cm<sup>2</sup> and 100% %R value was obtained at 0.006 A/cm<sup>2</sup> j value. The increase in current density

affected the oxidation of 3DES reactors more than in 2DES reactors.

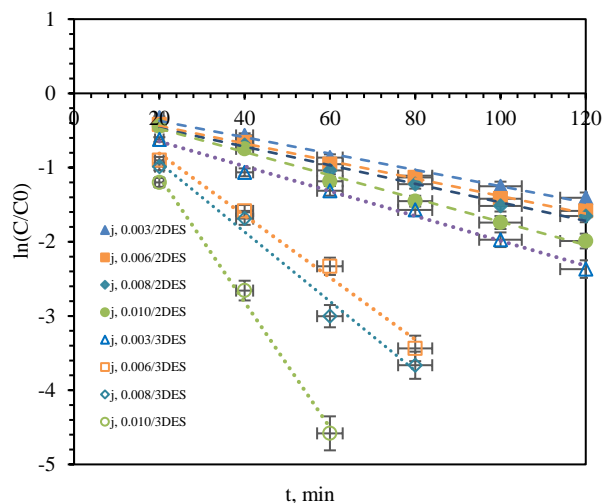


**Figure 7.** The pseudo-first-order kinetic model for 2DES and 3DES reactors at 0.003, 0.006, 0.008 and 0.010 A/cm<sup>2</sup> current density

When we evaluate the effect of current density from a kinetic point of view, the data obtained at all current densities were well compatible with the pseudo-first-order kinetic model with an R<sup>2</sup> value of 0.98-0.99. As the current density increased in 2DES reactors, the oxidative degradation rate increased, and the highest values of  $k_{1,2D}$  and  $k_{h,2D}$  were obtained as 0.0157 (min<sup>-1</sup>) and 0.01047 (cm/s) at 0.010 A/cm<sup>2</sup>, respectively. In 3DES reactors, the rate constant at 0.003 A/cm<sup>2</sup> was achieved as 0.0167 (min<sup>-1</sup>)  $k_{1,3D}$ , while at 0.010 A/cm<sup>2</sup>, it increased by approximately 5 times, reaching a value of 0.0845 min<sup>-1</sup>  $k_{1,3D}$ . Similarly, in 3DES reactors, when the current density increased from 0.003 A/cm<sup>2</sup> to 0.010 A/cm<sup>2</sup>, the mass transfer rate increased from 0.011 (cm/s) to 0.05633 (cm/s).

#### 4. Conclusions

In this study, activated carbon was produced from walnut shells by the chemical activation method. When potential differences between 2V and 4V are applied to 2DES and 3DES reactors containing MG solution, a higher % MG Removal was obtained in 3DES reactors than in 2DES reactors. In 3DES reactors, microelectrodes provide an extra surface for the oxidation of MG molecules. In this way, more MG molecules are degraded due to electron transfers occurring both on the carbon fibre

surface, which is the anode, and on the surface of the microelectrodes. In 3DES reactors, the energy consumption of 0.015, 0.028 and 0.048 kWh/gMG was realized for potential differences of 2, 3 and 4V. In 2DES reactors, the energy consumption of 0.020, 0.038, and 0.061 kWh/gMG occurred for the same potential differences. From this point of view, 3DES reactors are more economical.

When the potential difference is 4V, a value of 0.026 ( $\text{min}^{-1}$ )  $k_{1.3D}$  is obtained. In 3DES reactors, the rate constant at 0.003 A/cm<sup>2</sup> was achieved as 0.0167 ( $\text{min}^{-1}$ )  $k_{1.3D}$ , while at 0.010 A/cm<sup>2</sup>, it increased by approximately 5 times, reaching a value of 0.0845  $\text{min}^{-1}$   $k_{1.3D}$ . Similarly, in 3DES reactors, when the current density increased from 0.003 A/cm<sup>2</sup> to 0.010 A/cm<sup>2</sup>, the mass transfer rate increased from 0.011 (cm/s) to 0.05633 (cm/s). The change in current density in 3DES reactors had a more significant effect on the oxidative degradation rate of MG than the potential difference variation.

### Article Information Form

#### *Funding*

This study was financially supported by Eskişehir Osmangazi University Scientific Research Foundation (Project No: FBA-2021-1591).

#### *Authors' Contribution*

Conceptualization, Funding acquisition, Investigation, Methodology, Project administration, Resources, Validation, Visualization, Writing – review & editing.

#### *The Declaration of Conflict of Interest/ Common Interest*

The author has declared no conflict of interest or common interest.

#### *The Declaration of Ethics Committee Approval*

The author declares that this document does not require ethics committee approval or special permission.

#### *The Declaration of Research and Publication Ethics*

The author of the paper declares that he complies with the scientific, ethical, and quotation rules of

SAUJS in all processes of the paper and that she does not make any falsification of the data collected. In addition, she declares that Sakarya University Journal of Science and its editorial board are not responsible for any ethical violations that may be encountered and that this study has not been evaluated in any academic publication environment other than Sakarya University Journal of Science.

#### *Copyright Statement*

Authors own the copyright of their work published in the journal and their work is published under the CC BY-NC 4.0 license.

#### References

- [1] Wang, Z., Qi, J., Feng, Y., Li, K., Li, X., "Preparation of Catalytic Particle Electrodes from Steel Slag and Its Performance in a Three-Dimensional Electrochemical Oxidation System," *Journal of Industrial and Engineering Chemistry*, vol. 20, no. 5, 2014, pp. 3672–3677.
- [2] Tavares, M. G., Da Silva, L. V. A., Sales Solano, A. M., Tonholo, J., Martínez-Huitle, C. A., Zanta, C. L. P. S., "Electrochemical Oxidation of Methyl Red Using Ti/Ru<sub>0.3</sub>Ti<sub>0.7</sub>O<sub>2</sub> and Ti/Pt Anodes," *Chemical Engineering Journal*, vol. 204–206, 2012, pp. 141–150.
- [3] Isarain-Chavez, E., Baro, M. D., Rossinyol, E., Morales-Ortiz, U., Sort, J., Brillas, E., and Pellicer, E., "Comparative Electrochemical Oxidation of Methyl Orange Azo Dye Using Ti/Ir-Pb, Ti/Ir-Sn, Ti/Ru-Pb, Ti/Pt-Pd and Ti/RuO<sub>2</sub> Anodes," *Electrochimica Acta*, vol. 244, 2017, pp. 199–208.
- [4] Zhang, T., Liu, Y., Yang, L., Li, W., Wang, W., Liu, P., "Ti-Sn-Ce/Bamboo Biochar Particle Electrodes for Enhanced Electrocatalytic Treatment of Coking Wastewater in a Three-Dimensional Electrochemical Reaction System," *Journal of Cleaner Production*, vol. 258, 2020, p. 120273.

- [5] Xiao, H., Hao, Y., Wu, J., Meng, X., Feng, F., Xu, F., Luo, S., Jiang, B., "Differentiating the Reaction Mechanism of Three-Dimensionally Electrocatalytic System Packed with Different Particle Electrodes: Electro-Oxidation versus Electro-Fenton," *Chemosphere*, vol. 325, 2023, p. 138423.
- [6] Shen, B., Wen, X., Huang, X., "Enhanced Removal Performance of Estriol by a Three-Dimensional Electrode Reactor," *Chemical Engineering Journal*, vol. 327, 2017, pp. 597–607.
- [7] Sun, Y., Li, P., Zheng, H., Zhao, C., Xiao, X., Xu, Y., Sun, W., Wu, H., Ren, M., "Electrochemical Treatment of Chloramphenicol Using Ti-Sn/ $\gamma$ -Al<sub>2</sub>O<sub>3</sub> Particle Electrodes with a Three-Dimensional Reactor," *Chemical Engineering Journal*, vol. 308, pp. 1233–1242, 2017.
- [8] Li, J., Yan, J., Yao, G., Zhang, Y., Li, X., Lai, B., "Improving the Degradation of Atrazine in the Three-Dimensional (3D) Electrochemical Process Using CuFe<sub>2</sub>O<sub>4</sub> as Both Particle Electrode and Catalyst for Persulfate Activation," *Chemical Engineering Journal*, vol. 361, pp. 1317–1332, 2019.
- [9] Wang, Y., Cui, C., Zhang, G., Xin, Y., Wang, S., "Electrocatalytic Hydrodechlorination of Pentachlorophenol on Pd-Supported Magnetic Biochar Particle Electrodes," *Separation and Purification Technology*, vol. 258, p. 118017, 2021.
- [10] Ren, Y., Wang, J., Qu, G., Ren, N., Lu, P., Chen, X., Wang, Z., Yang, Y., Hu, Y., "Study on the Mechanism of High Effective Mineralization of Rhodamine B in Three Dimensional Electrochemical System with  $\gamma$ -Fe<sub>2</sub>O<sub>3</sub>@CNTs Particle Electrodes," *Separation and Purification Technology*, vol. 314, p. 123616, 2023.
- [11] Wang, X., Zhao, Z., Wang, H., Wang, F., Dong, W., "Decomplexation of Cu-I-Hydroxyethylidene-1,1-Diphosphonic Acid by a Three-Dimensional Electrolysis System with Activated Biochar as Particle Electrodes," *Journal of Environmental Sciences*, vol. 124, pp. 630–643, 2023.
- [12] Zhao, H.-Z., Sun, Y., Xu, L.-N., Ni, J.-R., "Removal of Acid Orange 7 in Simulated Wastewater Using a Three-Dimensional Electrode Reactor: Removal Mechanisms and Dye Degradation Pathway," *Chemosphere*, vol. 78, no. 1, pp. 46–51, 2010.
- [13] Chowdhury, S., Saha, P., "Sea Shell Powder as a New Adsorbent to Remove Basic Green 4 (Malachite Green) from Aqueous Solutions: Equilibrium, Kinetic and Thermodynamic Studies," *Chemical Engineering Journal*, vol. 164, no. 1, pp. 168–177, 2010.
- [14] Kumar, S., Singh, S., Srivastava, V. C., "Electro-Oxidation of Nitrophenol by Ruthenium Oxide Coated Titanium Electrode: Parametric, Kinetic and Mechanistic Study," *Chemical Engineering Journal*, vol. 263, pp. 135–143, 2015.
- [15] Al-Shannag, M., Al-Qodah, Z., Bani-Melhem, K., Qtaishat, M. R., Alkasrawi, M., "Heavy Metal Ions Removal from Metal Plating Wastewater Using Electrocoagulation: Kinetic Study and Process Performance," *Chemical Engineering Journal*, vol. 260, pp. 749–756, 2015.
- [16] Tonini, G. A., Ruotolo, L. A. M., "Heavy Metal Removal from Simulated Wastewater Using Electrochemical Technology: Optimization of Copper Electrodeposition in a Membraneless Fluidized Bed Electrode," *Clean Technologies and Environmental Policy*, no. 2, 2017, pp. 403–415, vol. 19.
- [17] Gottipati, R., Mishra, S., "Preparation of Microporous Activated Carbon from Aegle Marmelos Fruit Shell and Its Application in Removal of Chromium(VI) from Aqueous Phase," *Journal of Industrial and*

Engineering Chemistry, 2016, pp. 355–363, vol. 36.

- [18] Akbal, F., Camcı, S., “Copper, Chromium and Nickel Removal from Metal Plating Wastewater by Electrocoagulation,” *Desalination*, vol. 269, no. 1–3, pp. 214–222, 2011.
  
- [19] Meng, H., Chen, C., Yan, Z., Li, X., Xu, J., Sheng, G., “Co-Doping Polymethyl Methacrylate and Copper Tailings to Improve the Performances of Sludge-Derived Particle Electrode,” *Water Research*, vol. 165, p. 115016, 2019.